공학석사 학위논문

Circular polarization light dependent H_2O_2 generation by TiO_2 coated Helicoid

이산화 타이타늄 코팅된 헬리코이드에 의한 원편광 의존적 과산화수소 생성에 대한 연구

2022년 2월

서울대학교 대학원

재료공학부

김성호

Circular polarization light dependent H_2O_2 generation by TiO_2 coated Helicoid

지도 교수 남 기 태

이 논문을 공학석사 학위논문으로 제출함
2022년 2월

서울대학교 대학원
재료공학부
김 성 호

김성호의 공학석사 학위논문을 인준함
2022년 2월

위 원 장	김 진 영	(인)
부위원장	남 기 태	(인)
위 원	권 민 상	(인)

Abstract

Circular polarization light dependent H_2O_2 generation by TiO_2 coated Helicoid

Sungho Kim

Department of Materials Science and Engineering

The Graduate School

Seoul National University

Since the industrial revolution, various problems from fossil fuels have emerged, and new energy sources and eco-friendly production techniques are needed. In this context, H_2O_2 is an environmentally friendly chemical oxidizing agent that can be used for water treatment, etc. and a sustainable potential high energy carrier, so it is very important to produce it in an environmentally friendly way. For this purpose, a photocatalyst that uses solar fuel to send a photochemical reaction is promising. In particular plasmonic metal based photocatalysts are being actively studied as they enable the production of socially important sustainable energy sources and breakthroughs in the challenge of intrinsic photocatalysts such as the existing low efficiency and UV-limited photon absorption band. Although there are few in this context, the fascinating concept of chirality has recently been grafted here, and the development of advanced technology that enhances both efficiency and

controllability has shown the potential for extension to biochemical applications. However, the formation of a plasmonic photocatalyst structure with strong chiroptical was an obstacle, so further development in this field has hindered. Recently, our group successfully synthesized chiral single nanoparticle making unique 432-point group symmetry and helicoid morphology. Through chirality transfer in nanoscale utilizing organic-inorganic interactions, chiral gold nanoparticles with a g-factor of 0.2 are formed and named Helicoid. Using a sol-gel based titania coating method, uniform TiO_2 shell are successfully coated on the synthesized chiral gold nanoparticle and the thickness and uniformity of the TiO_2 shell could by easily controlled by adjusting the pH and time, respectively. Synthesized plasmonic metal–semiconductor nanocomposites can be directly applied as photocatalyst, which combine the plasmonic properties of the core and the photoactivity of the shell, thus improving the photocatalytic efficiency. By controlling various photocatalytic conditions, the H_2O_2 generation of Helicoid@TiO_2 photocatalyst achieved a high yield of 0.48mM and revealed several photocatalytic properties. A proposal of the applicability of our photocatalyst for the photo-dynamic therapy was conducted through an investigation of catalytic activity in the Vis-NIR region. Then, by controlling the handedness of the irradiation light, a demonstration of different hot electron injection process according to CPL was performed, and a remarkable CPL-dependent H_2O_2 generation was discovered for the first time.

Keywords: photocatalyst, H_2O_2 generation, polarization dependent photoreaction, Chiral plasmonic nanoparticle, Vis-NIR dirven photocatalyst

Student Number: 2020-21844

Contents

List of Figures

Chapter 1. Introduction

1.1 Conventional Method for Hydrogen Peroxide Production

H_2O_2, environmentally-friendly chemical oxidant used in pulp, paper bleaching, chemical synthesis, and water treatment, is a sustainable high potential energy carrier.[1] Industrial synthesis of H_2O_2 has been carried out through an anthraquinone process, which is a multi-step method requiring significant waste and energy.[1] To address this issue, direct synthesis of H_2O_2 from H_2 and O_2 for palladium-based materials has been studied. However, its practical application on large scale has been limited due to unsatisfactory production rates and selectivity, with potential explosion risk of H_2 and O_2 mixtures. Recently, as an alternative route, photocatalyzed synthesis of H_2O_2 drvien by sunlight has been highlighted as a H_2O_2 green fabrication.[2] Even without H_2, H_2O_2 can be produced in micromolar order O_2 saturated water under UV irradiation of TiO_2.[3] Various strategies such as hierarchical nanostructure, chemical modification, and heterostructure fabrication[4] have been presented to improve photocatalytic activity. Despite of tremendous efforts, there are still formidable challenges such as high recombination rate of charge carriers, low electron transfer rate, photon harvesting region limited in UV.

1.2 Plasmonic metal in photocatalyst

In recent years, developing photocatalysts based on plasmonic metal-semiconductor nanostructure has been a huge interest to extend the activity to the visible and NIR regions.[5] Localized surface plasmon resonance (LSPR) of plasmonic metal decays rapidly and generates energetic hot charge carriers through the nonradiative plasmon damping.[6] Hot electron with sufficient energy to cross the Schottky barrier transfer to semiconductor and participate in photochemical reactions.[7–9] Unique approach applied with above strategy to control photochemical reactions using circularly polarized light (CPL) has been introduced, although limited. In chiral environment, an intrinsically chiroplasmonic sensitive circular polarization dependent system may broaden its potential application to enatioselective photocatalysts in various fields. Kuang group showed that chiroplasmonic gold-gap-silver nanostructures(GGS NSs) increased the catalytic reaction rate with controlling CPL in the visible region. CPL coincides with the chiral direction of the GGS NSs could activate more hot electrons of chiral NPs, which led to the much higher catalytic activity in left-handed circular polarization (LCP) light than right-handed circular polarization (RCP) light and linearly polarization light.[10] Chen group reported chiral g-C_3N_4 based on chiral nematic cellulose nanocrystal films through silica templating exhibits hydrogen evolution variation when regulated with CPL.[11]

1.3 Objective of the thesis

Herein, we present chiral Helicoid@TiO_2 core-shell photocatalyst for visible-NIR-driven H_2O_2 generation modulated by CPL.(Figure 1.1) 432 helicoid III with exceptional intrinsic chiroptical activity has been chosen as core material in order to show the asymmetric response of the hot charges with respect to the handedness of CPL.[12] As semiconductior shell, titanium dioxide with photocatalytic properties along with its high resistance to photo corrosion has been selected. Using a sol-gel based titania coating method, uniform TiO_2 shell are successfully coated on the synthesized chiral AuNPs. Thickness and uniformity of the TiO_2 shell could by easily controlled by adjusting the temperature and TiO_2 precursor concentration. By controlling the several reaction condition, we could reveal the mechanism of H_2O_2 generation in chiral gold-silica hybrid photocatalyst. Under acidic environment with using ethanol as a hole scavenger, we achieved high H_2O_2 yield of 0.48 mM, which is 2 times higher than commercial TiO_2. Transfer of plasmon induced hot electorn to TiO_2 enable H_2O_2 generation in the visible and NIR regions. In addition, asymmetric H_2O_2 generation was demonstrated through different degrees of activation of the hot electron injection process according to CPL.

\

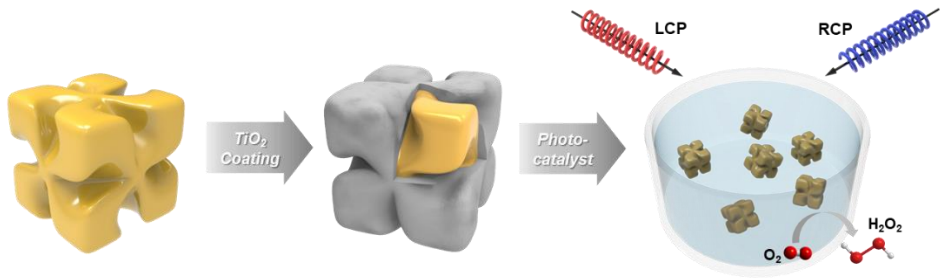

Figure 1. 1 Schmeatic illustration of plasmonic metal-semiconductor photocatalyst synthesis using Helicoid III template and CPL dependent H_2O_2 generation

Chapter 2. Experimental Procedure

2.1 Chemicals and materials

Tetrachloroauric(iii) trihydrate ($HAuCl_4 3H_2O$, 99.9%), Sodium borohydride ($NaBH_4$, 99%), Hexadecyltrimethylammonium bromide (CTAB, 99%), L-glutathione (γ-EC-G, 98%), L-ascorbic acid (99%), Titanium trichloride ($TiCl_3$, 15–20%) and sodium bicarbonate (≥99.7%) were purchased from Sigma-Aldrich and were used without further purification. High-purity deionized (DI) water (18.2 MΩ cm) was used in all of the procedures. Poly(sodium 4-styrenesulfonate) (PSS, MW = 70,000) was ordered from ACROS organics.

2.2 Methods

2.2.1 Synthesis of seed nanoparticles

Gold oxtahedral nanoparticles with a 80 nm edge length were synthesized as previously reported.[7] First, small spherical seeds (~2.5 nm) were prepared by the reduction of a $HAuCl_4 3H_2O$ aqueous solution (10 mM, 250 μl) with a $NaBH_4$ aqueous solution (10 mM, 800 μl) in a CTAC aqueous solution (100 mM, 1.3 ml). The spherical seeds were added to the growth solution containg the $HAuCl_4 3H_2O$ (10 mM, 200 μl) and CTAC (100 mM, 1.6 mL) aqueous solution,

and an ascorbic acid solution (100 mM, 950µl). After 15 min, the synthesized nanopartciels were washed by centrifugation (4000 rpm, 15min) and reapeat this step twice then, washed nanoparticles were dispered in 3mM CTAC solution.

2.2.2 Synthesis of peptide-directed chiral nanoparticles

The growth solution for 432 Helicoid III nanoparticles was prepared with 3.95ml DI water, 800 µl of 100mM CTAB and 200 µl of 10mM gold chloride trihydrate and stirred it for 10 seconds. Then 475 µl of 100mM ascorbic acid solution was added as color of solutionis changed from yellow to transparant. After 5 minutes incubation, L-glutathione solution and octahedral seeds were injected in order and stirred in each steps. After 2 hours incubation, the chiral gold nanopartciels solution expose purple color. It was washed twice by centrifugation (3000 rpm, 5min) and dispered in 1mM CTAB solution.

2.2.3 Synthesis of the Helicoid@TiO_2 photocatalyst \

Core–shell Helicoid@TiO_2 nanorods were prepared by a modified method. 200 µL of 17.1 wt% $TiCl_3$ containing 20 wt% HCl, was diluted by 6 mL of distilled water, followed by the addition of 1.2 mL of 0.93 M $NaHCO_3$. Then the PSS-encapsulated Au nanorods were immediately added in the mixture. After the hydrolysis reaction went for 30 min at room temperature, the as-obtained core/shell Helicoid@TiO_2 nanorods were collected by centrifugation twice and then dispersed

in 10 mL of water.

2.2.4 Photocatalytic study for H_2O_2 generation

The H_2O_2 evolution experiment was carried out in the following way. First, disperse our particles in an ethanol-DI solvent and react under O_2 purging, and strring under a certain amount of light for 3 hours.Then, H_2O_2 concentration was determined using an iodometric method. First of all, We adjusted the photocatalytic parameter with the aim of increasing the yield to see a distinct change when controlling the light. Second, we investigated the action spectrum and CPL dependence of our photocatalyst by controlling light. Detailed parameters of the photocatalytic experiment are described in the supplementary information.

2.2.5 Light penetration experiment dependent on porcine skin thickness

Porcine skins from Majang Livestock Market were used within 48 hours of slaughter. Cut the pig skin into 5mm*5mm and attach it to the front of the didoe as much as possible to minimize diffraction. And the distance is adjusted so that 60mW of light is irradiated based on the absence of pig skin in the middle. Short-wavelength lasers of 633 nm and 940 nm, respectively, are used as light sources in the visible and NIR regions. And when there is pig skin in the light path, measure the light intensity with a power-meter at a certain distance set above.

2.2.6 Characterization

The morphology of the Helicoid@TiO_2 NPs was characterized by scanning electron microscopy (SEM) micrographs were obtained using a Zeiss Supra 55 VP operating at 2 kV. Absorption spectra were collected on an ultraviolet-visible spectrophotometer (UNICO, UV2012C/PC/PCS).

Circular Dichroism Spectroscopy

Extinction and circular dichroism (CD) spectra were obtained using a J-815 spectropolarimeter instrument (JASCO).

Kuhn's dis-symmetry factor (g-factor) is a dimensionless quantity that is useful for quantitative comparisons of chiro-optical properties among different systems and was calculated from the measured extinction and CD values using:

$$g\text{-factor} = 2\frac{A_{\mathrm{L}} - A_{\mathrm{R}}}{A_{\mathrm{L}} + A_{\mathrm{R}}} \propto \frac{\mathrm{CD}}{\mathrm{extinction}}$$

Chapter 3. Results and Discussion

3.1 Synthesis of the Helicoid@TiO_2 photocatalyst

3.1.1 TiO_2 coating principle and mechanism on Helicoid

Two materials were used to design a plasmon system with powerful chiropactic activity. First, in the previous study, we successfully synthesized chiral single gold nanoparticle with good chiral activity that reacts differently according to LCP and RCP and name it 432 helicoid III. 432 helicoid III makes unique 432-point group symmetry and and helicoid morphology and a representative example achieved the highest g-factor of 0.2. Second, TiO_2 with good photocatalytic properties is widely used as a good photocatalyst for H_2O_2 production thanks to its nontoxic, cheap, economical, and stable for photo corrosion. To make the TiO_2 shell, we used $TiCl_3$, a trivalent precursor, not a commonly used tetravalent precursor.[13] Conventional Titanuim precursor such as TiF_4 and titanium alkoxides hydrolyze too fast, so $TiCl_3$, a precursor whose hydrolysis is relatively slower, is more effectively control the thickness and uniformity of the shell.

Figure 2.1 illustrates the formation process of TiO_2 shell-coated on Helicoid. Based on previous studies on core-shell nano heterostructure formation and functionalization with spherical gold nanoparticles, we induce the synthesis of a hybrid material that follows the surface of grafted chiral plasmonic object. First, the

prepared Helicoid stabilized with CTAB is subjected to ligand exchange with SDS, a negative charge modifier. By controlling the pH value, $TiCl_3$ is then hydrolyzed to $TiOH^{2+}$ and adsorbed to surface-modified Helicoid as a negative layer. Here, the electrostatic adsorption of titanium ions will allow the formation of a chiral characteristic metal-semiconductor photocatalyst with a Schottky barrier with the metallic component. Finally, Ti^{3+} species are oxidized to the TiO_2 shell at room temperature.

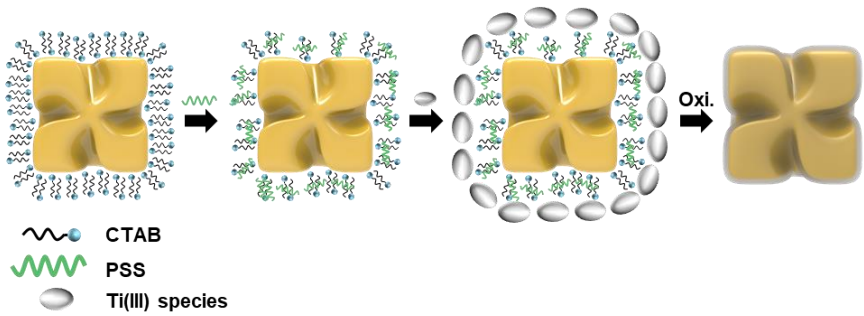

Figure 2. 1 Scheme of Helicoid@TiO_2 synthesis process

3.1.2 Parameters affecting TiO_2 shell uniformity and thickness

The as-prepared core–shell NPs are characterized by SEM (Figure 2.2). From the sem image, it can be seen that core–shell NPs with good dispersion and uniform mono-core morphologies were successfully synthesized. Different TiO_2 shell uniformity and thicknesses are obtained by controlling TiO_2 precursor concentration, temperature, pH, and water to ethanol ratio, reaction time, etc. As the TiO_2 precursor concentration increased, the shell became thicker.(Figure 2.3) At low concentrations, the shell layer only grows along the surface of the core, keeping the shell morphology the same as that of the core. However, at a concentration greater than 30 mM, the shell is isotropically thickened, crushing the morphology of the core and breaking the mono-core state. According to previous studies, pH and temperature increased, the TiO_2 hydrolysis rate increased.[14] By controlling the pH below 2.5 and the temperature close to 0 degrees respectively, it is facilitated to easily control TiO_2 shell formation at an appropriate kinectic rate without TiO_2 self nucleation. (Figure 2.3, S1) This allows the thickness of the TiO_2 shells can be controlled between 5 and 30nm and form nano island-like coating in which many small amorphous TiO_2 close aggregation. In addition, as the water to ethanol ratio raised, the TiO_2 condensation rate increased and the shell became massive.(Figure S2) Among them, we secured optimum conditions for Helicoid@ TiO_2 in which mono-core and coated 10 nm shell uniformly as shown in the Figure 2.2 and the H_2O_2 generation experiment was

conducted using this.

(A) **(B)**

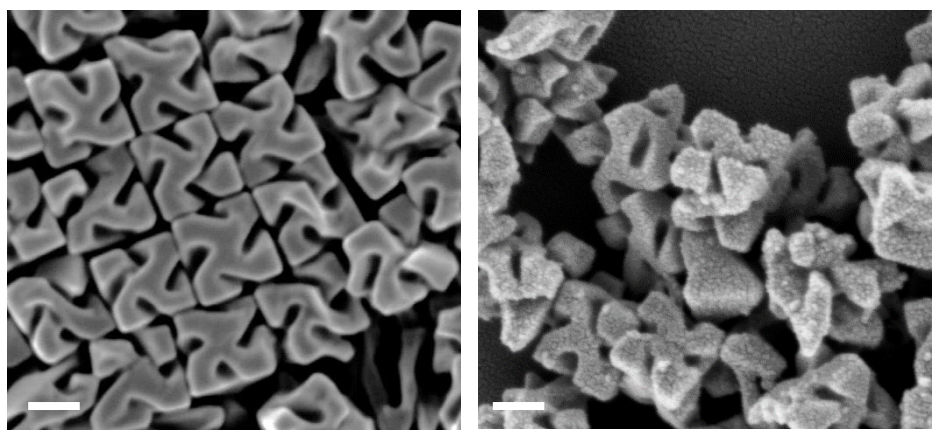

Figure 2. 2 Represntive SEM image of TiO_2 coating on Helicoid (A) before, (B) after (scale bar : 100nm)

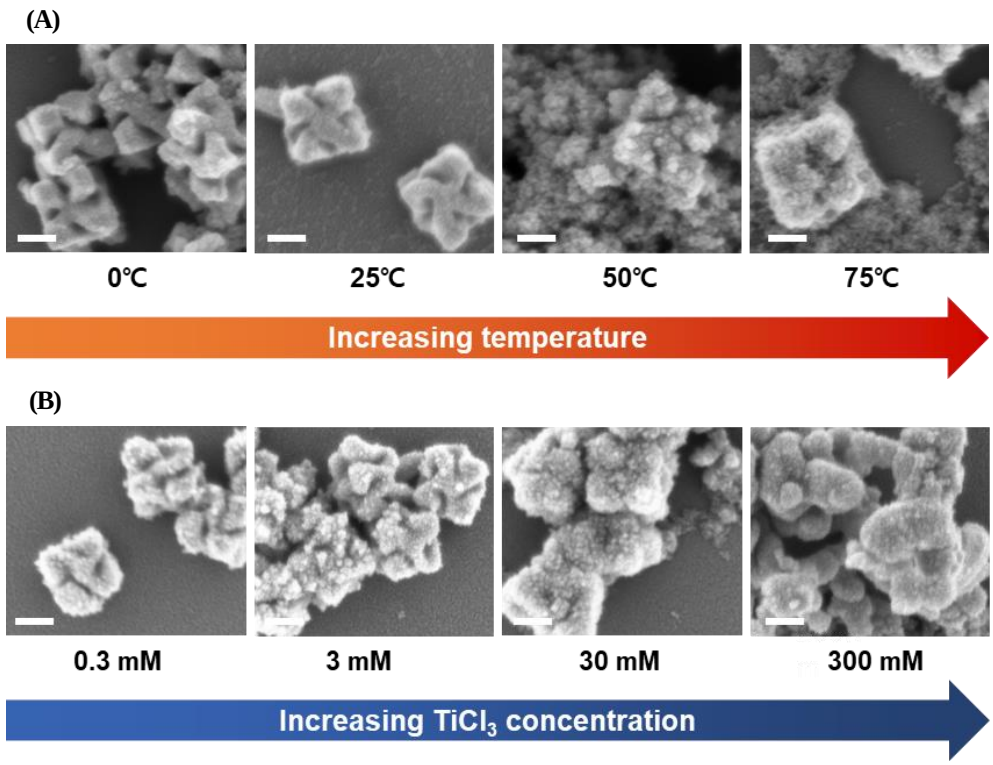

Figure 2. 1 (a) SEM image of effect of temperature on TiO_2 coating (b) effect of TiO_2 precursor concentration on TiO_2 coating (scale bar : 100nm)

3.2 Characterization of optimized conditions of the photocatalyted H_2O_2 generation by Helicoid@TiO_2 core-shell photocatalyst

3.2.1 Photocatalytic property depending on heat treatment

A photocatalytic experiment for H_2O_2 generation was performed using the prepared Helicoid@TiO_2 plasmonic metal semiconductor complex and ethanol as a hole scavenger under full spectrum light ($\lambda > 300$ nm) with a 300 W Xe lamp (power density = 100 mW cm−2). Several photocatalytic conditions were adjusted to reveal the photocatalytic characteristics of H_2O_2 generation of our particles. We find that the crystallinity of Helicoid@TiO_2 nanoparticles are largely affected by the heat treatment temperature. As shown in Figure 3.1, before thermal treatment, the TiO_2 shell shows an amorphous and porous structure. The catalytic activity of the heat treatment sample are obviously improved, compared to before treatment. It was observed that the amorphous TiO_2 shell was slightly crystallized, boosting the charge transfer, thus increasing the yield. On the other hand, when heat of 170 degrees or higher is applied, the particles cannot withstand the heat and are deformed, resulting in a small specific surface area and a sharp decrease in catalytic activity.

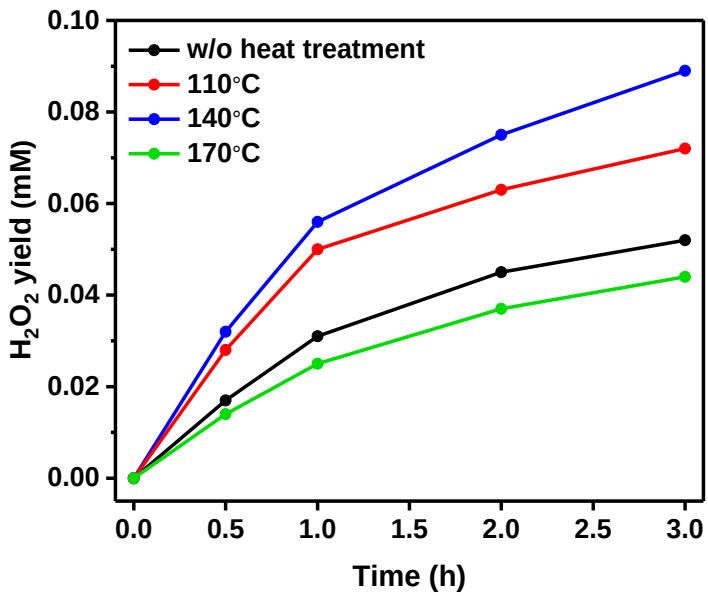

Figure 3. 1 Time course of H_2O_2 photoproduction dependent on heat treatment temperature

3.2.2 Photocatalytic property dpending on purging and pH

The effect of proton concentrations on H_2O_2 formation are shown in Figure 2.2. H_2O_2 yield increased with time as the pH value decreased, and in particular, it increased rapidly when changing from pH 5 to 3. The highly pH dependent H_2O_2 production indicated that the H_2O_2 generation was regulated by the proton-coupled electron transfer mechanism. The accelerated H_2O_2 generation with the decrease of pH vaule could be attributed to the enhanced desorption of H_2O_2 on the surface of TiO_2. In addition, we previously found that the H_2O_2 in our system is generated through O_2 reduction through purging environment experiments.(Figure 3.2) Comprehensively, it suggests that the superoxide radical, which is a typical intermediate of the 2 electron O_2 reduction reaction path for H_2O_2 production at high proton concentration, is stabilized.[15]

(A)

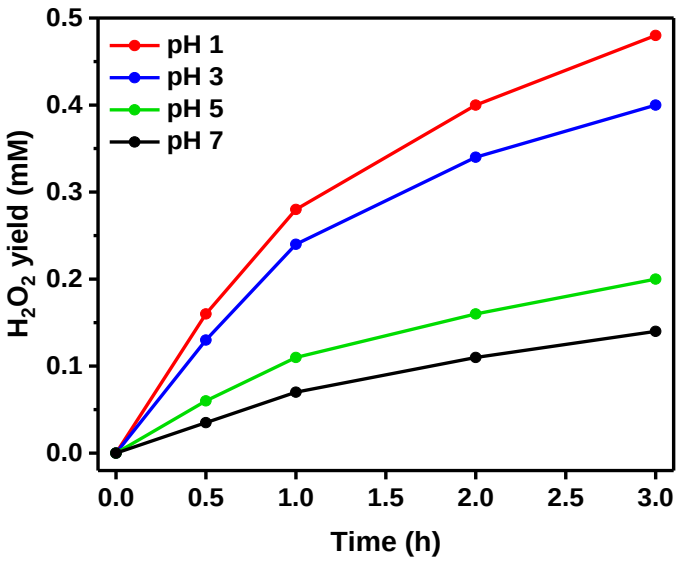

(B)

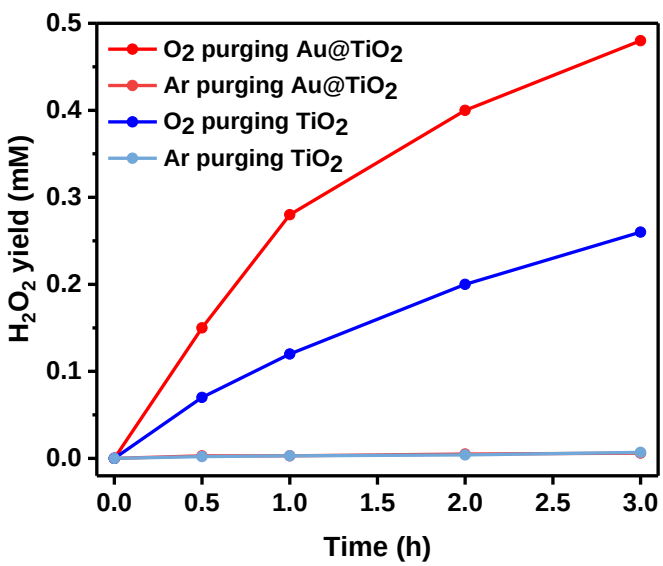

Figure 3. 2 Time course of H_2O_2 photoproduction dependent on (A) pH (B) purging and comparsion with TiO_2

3.2.3 Photocatalytic durabiiltiy

We could see the yield aspect according to the concentration. As the concentration increased, the number of particles increased, but the scattering of light also increased, so the number of photons absorbed per particle decreased. Therefore the H_2O_2 yield was saturated above a certain level. Finally, we achieved a maximum yield of 0.48mM h^{-1}. This is 2 times larger than commercial TiO_2 under the same conditions. The recyclability of the catalysts was also studied.(Figure 3.3) Four cycles were carried out and each photocatalytic cycle was conducted for 3h. After each photocatalysis run, the catalyst was collected from the reaction solution by centrifugation and then subjected to the next photocatalytic reaction As the cycle was repeated, the yield decreased and in the 4th cycle, it was saturated to half the maximum yield. Our photocatalyst was able to withstand relatively harsh conditions and evaulated its performance maintenance over repeated cycles.

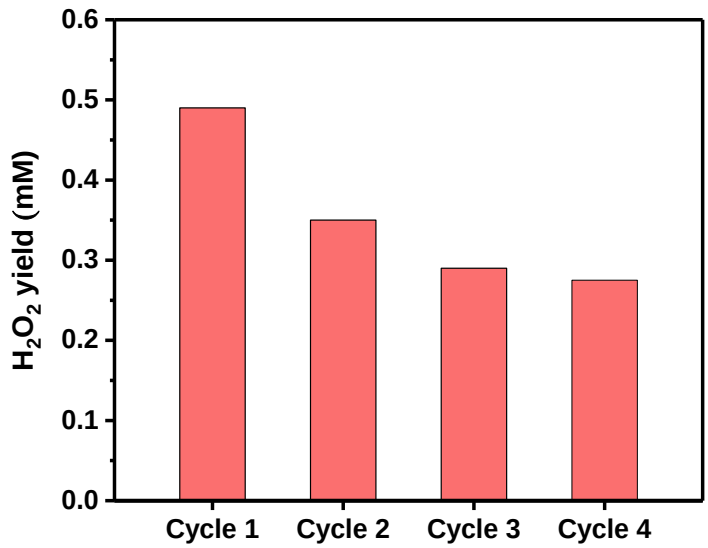

Figure 3. 3 Durability of photoproduction of H_2O_2

3.3 Investigation of catalytic activity depending on function of light

3.3.1 Investigation of catalytic activity in Vis-NIR region

After sufficiently increasing the yield, we conducted H_2O_2 generation experiment by controlling the light. First, using a band pass filter, we controled the irradiation region of light and investigated the catalytic activity of each region. Under the same 80mWcm^{-2} light irradiation in each region, yields of 0.33, 0.058, and 0.048mM h^{-1} were obtained in the UV, Vis, and NIR regions, respectively.(Figure 4.1) Existing photocatalysts were usually operated in the UV region. UV is only 5% of sunlight, so a system using only UV has a limit in reaction efficiency. According to the result, the interparticle optical coupling originated from the chiral inorganic plasmonic resonators leads to strong chiroptical activities in the Vis-NIR range of the electromagnetic spectrum. More specifically, in our hot electron generation mechanism, an excited high-energy electron distribution that is sufficiently larger than the Fermi level of the metal is generated by electromagnetic activation. (Figure 4.1) These energetic electrons transfer across the Schottky barrier by overbarrier or tunneling near the interface of the heterostructure and are injected into the TiO_2 component. In addition, in the Helicoid@TiO_2 heterostructure, TiO_2 accelerates electron hole speration and prolongs the hot electron lifetime, and acts as an active site.

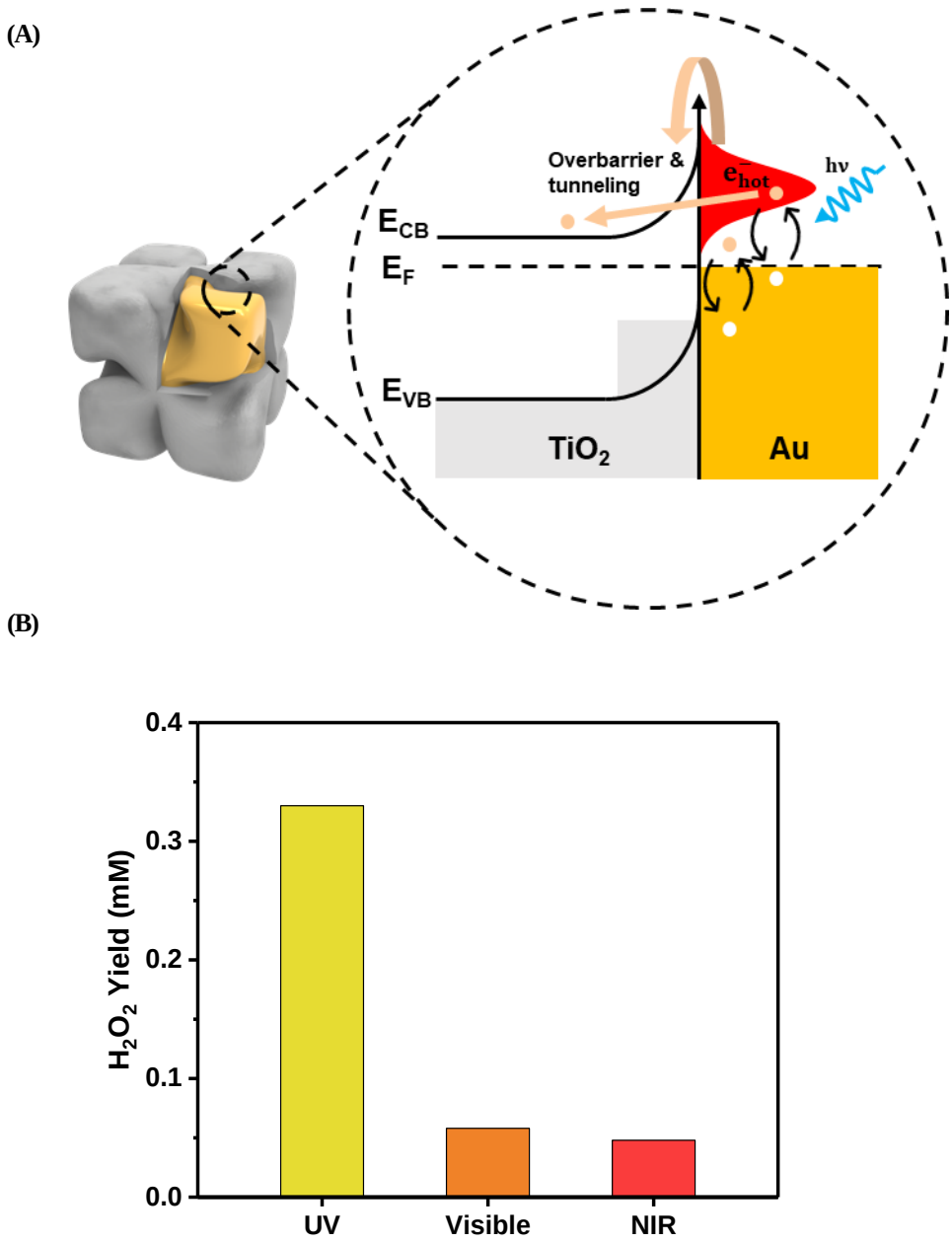

Figure 4. 1 (A) Scheme of plamon induced hot electorn injection process (B)

Photocatalytic activity dependent on irradiation light range

3.3.2 Investigation of catalytic activity depending on CPL

Given the physical interface created between the metal and semiconductor components and the chiroptical activities, these hybrids are ideal candidates for polarization-sensitive photocatalytic reactions. To perform this experiment, we synthesized high/low g-factor Helicoid@ TiO_2 by adjusting the chirality so that the maximum g-factor wavelength is the same.(Figure 4.2) 633 nm short wavelength laser corresponding to the hybrid plasmon range was used as a light source, and left or right circular polarizer quarter wave plate was inserted into the path of the light source. We then evaluated the H_2O_2 photocatalyted yield as a function of irradiation time in the presence of one of two different g-factors of Helicoid@TiO_2, using the modified lamp described above as the CPL source. When a photocatalytic reaction was performed using a low g-factor Helicoid@TiO2 as a photocatalyst under RCP excitation, an activity value greater than 2.9% was observed compared to the activity value for an irradiation source with opposite polarization. Similarly, when high g-factor Helicoid@ TiO_2 is activated using RCP light, 7.4% greater activity value is observed compared to the activity value corresponding to LCP under the same conditions.(Figure 4.2) Depending on the CPL handedness, the plasmonic excited electrons exhibit an asymmetric responce, which may enable polarization-sensitive photocatalysis. Consequently, when the handedness of the incoming CPL and the helicity of the substrate match, the plasmon induced hot electron injection can be

activated compared to the opposite handedness CPL, leading to efficient production of the product.[16] Also, these data clearly demonstrate that by tuning the chirality of the core, it can directly affect the population of generated high-temperature charges and furthermore control the controability of the photoreaction. Our chiral plasmonic metal-semiconductor heterostructure template with easily adjustable chirality enables rapid real-time control of photochemical reactions in-situ without increasing the amount of light, and is expected to have great potential in vivo.

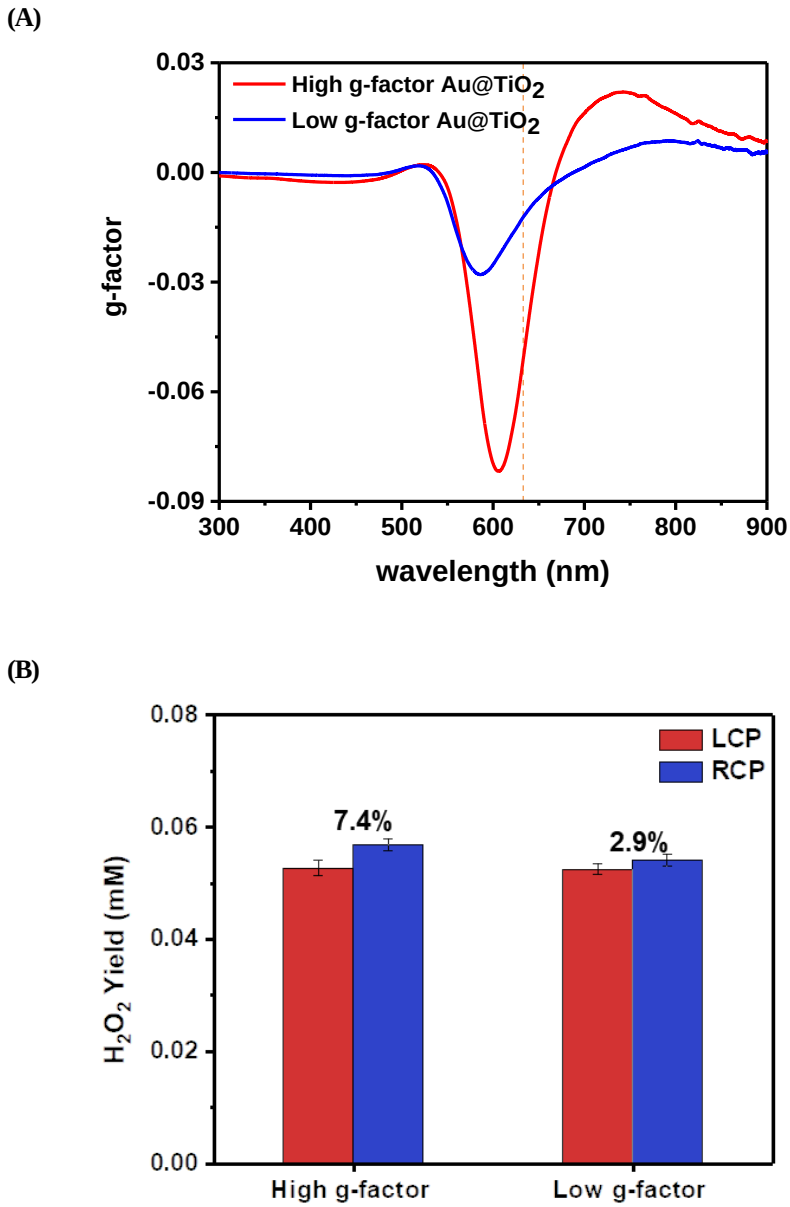

Figure 4. 2 (A) Circular dichroism spectra of high/low Helicoid@TiO_2 (B) Photocatalytic H_2O_2 generation of Helicoid@TiO_2 under LCP/RCP

3.3.3 Proposal of the applicability of the Helicoid@TiO_2 photocatalyst for photo dynamic therapy

To summarize the advantages of our photocatalyst, first, H_2O_2 is generated in Vis-NIR, and secondly, TiO_2 is coated in the nano islands form. NIR is used in phototherapy due to its good penetration rate into skin and low phototoxicity. In addition, our NIR drivien photocatalyst has room for use in cancer treatment using the characteristics of cancer cells that are more vulnerable to ROS stress than normal cells. Also, our particles are in the form of nano-islands rather than whole core shells, so it is convenient to functionalize for bare Au. By attaching to Au by functionalizing an antibody that strongly interacts with the body on the surface of cancer cells, selective tumor targeting will be possible. Utilizing the these advantages, our photocatalyst can be applied to photo dynamic therapy.

In order to confirm the applicability of NIR as photo dynamic therapy, we conducted a penetration test with pig skin, which is the most similar to human skin. The transmission rate was measured with a light power-meter by irradiating 2, 3, and 4 mm pig skin specimens within 48 hours of slaughtering with 633 nm in the visible region and 940 nm in the NIR region.(Figure 5) At 2mm thickness, light was transmitted 1.05% at 940nm and 0.15% at 633nm, and the NIR transmission rate was 5~6 times higher for all thicknesses.(Figure 5) As the thickness increased, the transmission rate tended to decrease, and in both wavelength bands, 2mm was about twice as large as 4mm. In the reference of previous studies, it was confirmed that

940nm, the target light wavelength of our photocatalyst, has room to operate within the skin, when looking at the transmission rate of 0.1% to 5% depending on the light wavelength, waveform tuning, and skin type and material.

(A)

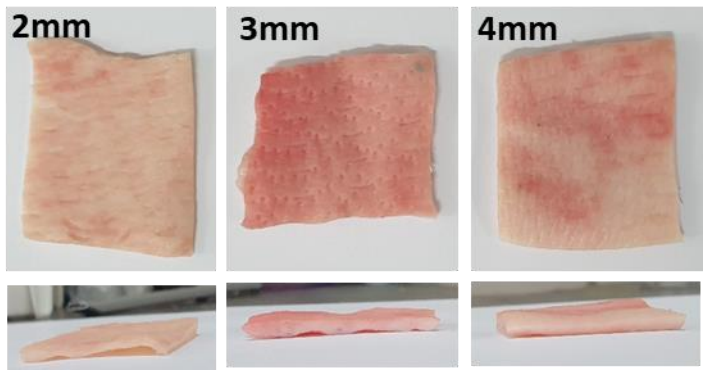

(B)

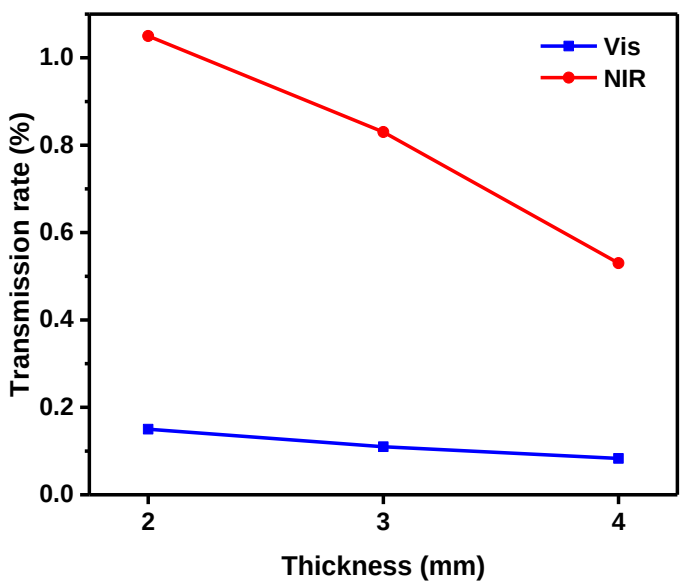

Figure 5. 1 (A) 2, 3, 4mm thickness of porcine skin (B) Tramission rate dependent on porcine skin thickness under Vis/NIR

Chapter 4. Concluding Remarks

Polarization-dependent H_2O_2 generation using chiral plasmonic metal-semiconductor heterostructure template was demonstrated for the first time. Helicoid@TiO_2 core-shell photocatalyst was successfully synthesized by sol-gel based titania coating method for H_2O_2 green fabrication by O_2 reduction. High yield of 0.48 mM was achieved by controlling photocatalytic condition. The design of a photocatalytic sensitive circular polarization dependent process may broaden its potential application to photocatalysts in biological and chemical physics. Hybrid photocatalyst operated in Vis-NIR region through plasmon induced hot electron hot injection, extending its applicability for photo dynamic therapy. This chiroptical plasmon system engineering and cpl dependence photocatalytic regulation strategy will help us to better understand the generation of H_2O_2 and promise great potential for a wide range of new applications, such as photodynamic therapy using ROS.

References

1. Campos-Martin, J. M.; Blanco-Brieva, G.; Fierro, J. L. G. Hydrogen Peroxide Synthesis: An Outlook beyond the Anthraquinone Process. *Angew. Chemie Int. Ed.* **2006**, *45* (42), 6962–6984.
2. Zhuang, H.; Yang, L.; Xu, J.; Li, F.; Zhang, Z.; Lin, H.; Long, J.; Wang, X. Robust Photocatalytic H2O2 Production by Octahedral Cd3(C3N3S3)2 Coordination Polymer under Visible Light. *Sci. Rep.* **2015**, *5* (1), 16947.
3. Li, X.; Chen, C.; Zhao, J. Mechanism of Photodecomposition of H 2 O 2 on TiO 2 Surfaces under Visible Light Irradiation. *Langmuir* **2001**, *17* (13), 4118–4122.
4. Wu, Q.; Cao, J.; Wang, X.; Liu, Y.; Zhao, Y.; Wang, H.; Liu, Y.; Huang, H.; Liao, F.; Shao, M.; et al. Author Correction: A Metal-Free Photocatalyst for Highly Efficient Hydrogen Peroxide Photoproduction in Real Seawater. *Nat. Commun.* **2021**, *12* (1), 1187.
5. Liu, J.; Feng, J.; Gui, J.; Chen, T.; Xu, M.; Wang, H.; Dong, H.; Chen, H.; Li, X.; Wang, L.; et al. Metal@semiconductor Core-Shell Nanocrystals with Atomically Organized Interfaces for Efficient Hot Electron-Mediated Photocatalysis. *Nano Energy* **2018**, *48*, 44–52.
6. Furube, A.; Hashimoto, S. Insight into Plasmonic Hot-Electron Transfer and Plasmon Molecular Drive: New Dimensions in Energy Conversion and Nanofabrication. *NPG Asia Mater.* **2017**, *9* (12), e454–e454.

7. Ahlawat, M.; Mittal, D.; Govind Rao, V. Plasmon-Induced Hot-Hole Generation and Extraction at Nano-Heterointerfaces for Photocatalysis. *Commun. Mater.* **2021**, *2* (1), 114.

8. Sousa-Castillo, A.; Comesaña-Hermo, M.; Rodríguez-González, B.; Pérez-Lorenzo, M.; Wang, Z.; Kong, X.-T.; Govorov, A. O.; Correa-Duarte, M. A. Boosting Hot Electron-Driven Photocatalysis through Anisotropic Plasmonic Nanoparticles with Hot Spots in Au–TiO 2 Nanoarchitectures. *J. Phys. Chem. C* **2016**, *120* (21), 11690–11699.

9. Zhang, Y.; He, S.; Guo, W.; Hu, Y.; Huang, J.; Mulcahy, J. R.; Wei, W. D. Surface-Plasmon-Driven Hot Electron Photochemistry. *Chem. Rev.* **2018**, *118* (6), 2927–2954.

10. Hao, C.; Xu, L.; Ma, W.; Wu, X.; Wang, L.; Kuang, H.; Xu, C. Unusual Circularly Polarized Photocatalytic Activity in Nanogapped Gold-Silver Chiroplasmonic Nanostructures. *Adv. Funct. Mater.* **2015**, *25* (36), 5816–5822.

11. Lin, W.; Hong, W.; Sun, L.; Yu, D.; Yu, D.; Chen, X. Bioinspired Mesoporous Chiral Nematic Graphitic Carbon Nitride Photocatalysts Modulated by Polarized Light. *ChemSusChem* **2018**, *11* (1), 114–119.

12. Lee, H.-E.; Ahn, H.-Y.; Mun, J.; Lee, Y. Y.; Kim, M.; Cho, N. H.; Chang, K.; Kim, W. S.; Rho, J.; Nam, K. T. Amino-Acid- and Peptide-Directed Synthesis of Chiral Plasmonic Gold Nanoparticles. *Nature* **2018**, *556* (7701), 360–365.

13. Chen, T.-M.; Xu, G.-Y.; Ren, H.; Zhang, H.; Tian, Z.-Q.; Li, J.-F. Synthesis of Au@TiO 2 Core–Shell Nanoparticles with Tunable Structures for Plasmon-Enhanced Photocatalysis. *Nanoscale Adv.* **2019**, *1* (11), 4522–4528.

14. Cassaignon, S.; Koelsch, M.; Jolivet, J.-P. From TiCl3 to TiO2 Nanoparticles (Anatase, Brookite and Rutile): Thermohydrolysis and Oxidation in Aqueous Medium. *J. Phys. Chem. Solids* **2007**, *68* (5–6), 695–700.

15. Zheng, L.; Su, H.; Zhang, J.; Walekar, L. S.; Vafaei Molamahmood, H.; Zhou, B.; Long, M.; Hu, Y. H. Highly Selective Photocatalytic Production of H2O2 on Sulfur and Nitrogen Co-Doped Graphene Quantum Dots Tuned TiO2. *Appl. Catal. B Environ.* **2018**, *239*, 475–484.

16. Hao, C.; Gao, R.; Li, Y.; Xu, L.; Sun, M.; Xu, C.; Kuang, H. Chiral Semiconductor Nanoparticles for Protein Catalysis and Profiling. *Angew. Chemie* **2019**, *131* (22), 7449–7452.

국 문 초 록

이산화 타이타늄 코팅된 헬리코이드에 의한 원편광 의존적 과산화수소 생성에 대한 연구

산업혁명 이후 화석연료의 다양한 문제가 대두되면서 새로운 에너지원과 그에 대한 친환경적인 생산기술이 요구되고 있다. 이러한 맥락에서 과산화수소는 종이 표백, 화학 합성, 폐수 처리 등에 사용될 수 있는 친환경적인 화학적 산화제이자 지속가능한 잠재적인 고에너지 운반체이다. 기존 과산화수소를 합성 방법들은 많은 에너지와 비용, 위험성을 동반하기 때문에 이를 대체할 경제적이고 친환경적 대체합성 방안들이 활발히 연구되어지고 있다. 그 중 태양 연료를 사용하여 광화학 반응을 보내는 광촉매가 다른 방법들보다 친환경적이기 때문에 큰 경쟁력이 있다. 특히 플라즈모닉 금속 기반 광촉매는 사회적으로 중요한 지속 가능한 에너지원의 생산을 가능하게 하고 기존 광촉매의 고유의 한계를 돌파 가능하기 때문에 큰 관심을 받아왔다. 그리 많지 않지만, 최근 키랄성 개념을 플라스모닉 급속에 접목시켜 효율성과 제어 가능성을 모두

향상시키는 전략이 소개되었고 더 나가 생화학 응용 분야로의 확장 가능성을 보여주었다. 그러나 이 전략은 강한 키랄 광학 성질을 갖는 플라즈모닉 나노 구조체 형성이 어려워 이 전략을 사용한 발전이 더디게 되었다. 또한 아직까지 과산화수소 같은 유의미한 에너지원을 이런 전략을 통해서 생성 및 조절한 예시는 없다.

우리는 카이랄 플라즈모닉 금속-반도체 나노복합체 디자인을 통해 편광 의존적 과산화수소 생성을 처음 발견하였다. 이러한 발견은 헬리코이드@이산화티타늄 광촉매의 성공적인 합성에 의해 구현 가능하였는데 이를 위해 2가지 물질을 선택하였다. 첫번째는 우리 그룹에서 합성한 독특한 432 점 그룹 대칭과 나선 형태를 만드는 키랄 단일 금 나노 입자이다. 유기-무기 상호작용을 활용한 나노 규모의 키랄성 전달을 통해 g-factor가 0.2인 키랄 금 나노입자를 합성하였고 이를 헬리코이드라고 명명하였다. 두번째는 독성이 없고 저렴하고 경제적이며 광부식에 안정적이고 광촉매 특성에 좋아 과산화수소 생산을 위한 우수한 광촉매로 알려진 이산화티타늄이다. 플라즈모닉 금속인 헬리코이트를 중심으로, 광촉매 특성이 좋은 이산화티타늄을 껍질로 하여, 솔-겔 기반의 티타니아 코팅 방법을 통해 균일한 이산화티타늄 껍질을 코팅된 헬리코이드@이산화티타늄 나노 입자를 성공적으로 합성하였다. 껍질 형성에 영향을 미치는 파라미터를 세분화 하여, 각 요소별 영향에 대해서 탐구

하였고, 이산화티타늄 껍질의 두께와 균일성은 각각 전구체 농도, 온도 등을 조정하여 균일도와 두께를 단계별로 조절하였다. 이런 방식으로 최적화된 합성 방법을 기반으로 pH 등 여러 광촉매적 실험조건을 조절하여 0.48mM 이라는 높은 과산화수소 활성을 달성하였다. 그리고 파장별 촉매 활성 조사를 통해 가시광과 근적외선 영역에서 활성을 가짐을 확인하였다. 이어 조사광의 원형편광 방향을 제어하여 원형편광에 따른 서로 다른 열전자주입과정이 촉매 활성에 영향을 미친다는 것을 발견하였고 원형편광 의존적 과산화수소 발생을 처음 관찰하였다. 이러한 우리 광촉매의 특징을 바탕으로 광역학요법로서의 적용처를 제시하였다.

본 연구에서 개발된 자외선 뿐만 아니라 가시광-근적외선 영역대에서 구동하는 플라즈모닉 기반 광촉매 플렛폼은, 새로운 맞춤형 특성을 위한 용액 기반 금속-반도체 나노 이종구조체 제작 기반 기술로 사용될 것이라 생각하며, 플라즈모닉 나노구조체의 생화학 분야로서의 적용가능성을 확대해 줄 수 있을 것이라 생각한다.

주요어: 광촉매, 과산화수소, 편광 의존적 광반응, 키랄 플라즈몬 나노입자, 가시광-근적외선 구동 광촉매
학번: 2020-21844